

RESEARCH ARTICLE

## Synthesis of $\text{Li}(\text{Ni}_{1/3}\text{Mn}_{1/3}\text{Co}_{1/3})\text{O}_2$ by Glycine Nitrate Combustion Process

T.H.N.G. Amaraweera<sup>1,2</sup>, Deshapriya Senarathna<sup>1</sup> and Athula Wijayasinghe<sup>1,\*</sup>

<sup>1</sup>National Institute of Fundamental Studies, Hantana Road, Kandy, Sri Lanka

<sup>2</sup>Department of Science and Technology, Uva Wellassa University, Badulla, Sri Lanka

Received: 12/10/2016; Accepted: 01/11/2016

**Abstract:** Glycine Nitrate Combustion (GNC) method was successfully employed for the synthesis of  $\text{Li}(\text{Ni}_{1/3}\text{Mn}_{1/3}\text{Co}_{1/3})\text{O}_2$  with powder characteristics appropriate for the cathode of rechargeable Li-ion batteries (LIBs). The outcome of this study proposed an optimum value of 0.6 for the Glycine: Nitrate ratio to obtain phase pure, well crystalline and rather spherical shaped  $\text{Li}(\text{Ni}_{1/3}\text{Mn}_{1/3}\text{Co}_{1/3})\text{O}_2$  micron size secondary particles by the GNC process. These secondary particles were composed of softly agglomerated primary particles of 200 - 300 nm in size. This particle morphology is regarded as a highly favorable for the functioning as a cathode in LIB. The electrical conductivity of  $\text{Li}(\text{Ni}_{1/3}\text{Mn}_{1/3}\text{Co}_{1/3})\text{O}_2$ , determined by the dc four-probe technique, revealed the semiconducting nature with conductivity of the order of  $10^{-7} \text{ S cm}^{-1}$ , at 25 °C. Lithium ion half-cell constructed with this prepared cathode material showed initial discharge capacity of  $187 \text{ mAhg}^{-1}$  with irreversible capacity of  $25 \text{ mAhg}^{-1}$  at C/5 rate with a cut-off voltage of 2.5 - 4.6 V, at 25 °C. This performance can be attributed to the highly favorable particle morphology obtained by the successful use of GNC process for the powder synthesis.

**Keywords:** glycine nitrate combustion method, powder morphology,  $\text{Li}(\text{Ni}_{1/3}\text{Mn}_{1/3}\text{Co}_{1/3})\text{O}_2$ , cathode material, Li-ion rechargeable battery.

### INTRODUCTION

Particle morphology can play a critical role on the performance of an electrode material, especially in the electrochemical cells such as rechargeable batteries, fuel cells ...etc. Therefore, in developing electrodes for electrochemical cells, a greater attention has to be paid on optimizing the particle morphology of the electrode materials. Among the currently evolving rechargeable batteries, the Lithium ion battery (LIB) is the highly promising source of portable energy. However, in order to make it

more competitively priced, performance enhanced and durable, special attention has to be paid to develop its electrode system. In the development of electrodes for LIBs, much attention has been paid on its cathode and especially the morphology of the cathode material (Liu *et al.*, 2014; Oljaca *et al.*, 2014; Samarasingha *et al.*, 2008). Cathode materials with sub-micron size particles with primary nano-scale particles were proposed as promising cathode materials for LIB due to the disadvantage of nano sized particles (Oljaca *et al.*, 2014; Shi *et al.*, 2013, Zhang, 2007; Liu *et al.*, 2014). The method of synthesis and its condition will play a very important role on determining morphology of powder particles. Therefore a number of different synthesis methods and routes have so far been investigated for synthesizing cathode materials for the LIB (Chick *et al.*, 1990; Samarasingha *et al.*, 2008).

The Glycine Nitrate Combustion (GNC) method involves formation of a chemically homogenous precursor and auto-combustion resulting in a short calcination time and highly crystalline nano-scale powder particles (Wilcox *et al.*, 2009; Wijayasinghe, 2006; Patoux, 2004). Further, the size and morphology of powder particles synthesized by GNC process depend critically on the fuel to oxidant ratio, cation concentration to fuel ratio and the amount and evolution rate of the gases released during the combustion process (Chick, 1990). However, investigations have not yet been carried out to study the effect of the ratio of fuel glycine to the oxidized metal nitrate, in relation to the synthesis of  $\text{Li}(\text{Ni}_{1/3}\text{Mn}_{1/3}\text{Co}_{1/3})\text{O}_2$ , which is presently a highly promising candidate for LIB cathode. It is expected that the optimization of this Glycine:Nitrate (G:N) ratio may result in powder

\*Corresponding Author's Email: [athula@ifs.ac.lk](mailto:athula@ifs.ac.lk)

particles with more desirable characteristics. By considering these factors, the present study involved with optimizing the GNC method, by investigating the effect of Glycine:Nitrate ratio on powder properties. By doing so, it was aimed to obtain  $\text{Li}(\text{Ni}_{1/3}\text{Mn}_{1/3}\text{Co}_{1/3})\text{O}_2$  powders with particle morphology and other characteristics appropriate for Li-ion battery cathode application.

## EXPERIMENTAL

### Powder synthesis by the GNC method

For this study,  $\text{Li}(\text{Ni}_{1/3}\text{Co}_{1/3}\text{Mn}_{1/3})\text{O}_2$  powders were synthesized by the GNC method at different Glycine to Nitrate ratios. In this method, stoichiometric amount of metal nitrates,  $\text{LiNO}_3$ ,  $\text{Ni}(\text{NO}_3)_2 \cdot 6\text{H}_2\text{O}$ ,  $\text{Co}(\text{NO}_3)_2 \cdot 6\text{H}_2\text{O}$  and  $\text{Mn}(\text{NO}_3)_2 \cdot 4\text{H}_2\text{O}$  (Merck, Germany) were mixed with distilled water. Glycine as a fuel for combustion was added to the nitrate solution and the new powder samples were prepared with various Glycine to Nitrate ratios (G:N) in the range from 0.2 to 1.5, to investigate the effect of G:N on the powder properties. The precursor solution was thoroughly mixed using a magnetic stirrer hotplate at room temperature for two hours. Then it was mixed at 60 °C for one hour and at 100 °C another one hour. Then the solution temperature was increased stepwise (25 °C) from 100 °C to 300 °C. During this process, the resultant viscous liquid ignited and underwent self-sustaining combustion producing an ash composed of the oxides. Finally, the ash product was further calcinated at 900 °C in air for two hours, to obtain the final oxide product.

### Powder characterization

X-ray powder diffraction (XRD, Siemens D5000) using Cu K- $\alpha$  radiation was used for phase identification and specially to identify the crystalline nature of the synthesized materials. Scanning electron microscopy (SEM, FEI Quanta 200 FEG-ESEM) was employed to study the particle size and morphology of synthesized powders. Thermogravimetric analyses (TGA) were carried out using a Perkin-Elmer TGS-2 Thermogravimetric System. For that, calcinated powders (0.5 mg) were heated up to 800 °C in a platinum pan at a heating rate of 5 °C min<sup>-1</sup>, under nitrogen atmosphere.

### Powder densification and electrical characterization

In order to find the optimum pressing conditions for solid pellets, the calcinated powders were uni-axially pressed by applying pressures in the range from 50 MPa to 350 MPa. Green pellets of 12 mm in diameter and 0.5 mm thick were pressed and subsequently sintered at 1000 °C for two hours, in air. For the electrical conductivity measurements, the flat end surfaces of the sintered pellets were gold pasted (G3535, Agar Scientific Ltd., England) in order to improve the contact between the specimen pellets and the sample holder. The *d.c.* four probe electrical conductivity measurements were performed on the sintered pellets on heating and cooling in the temperature range between 25 and 200 °C, keeping the specimens in a sample holder, inside a pot furnace.

## RESULTS AND DISCUSSION

### Phase analysis

In the GNC process, the metal nitrate acts as the oxidant while glycine supplies fuel for the combustion reaction (Chick, 1990). Therefore, in order to study the effect of Glycine to Nitrate ratio (G:N), on the powder morphology, few different  $\text{Li}(\text{Ni}_{1/3}\text{Co}_{1/3}\text{Mn}_{1/3})\text{O}_2$  powder batches were prepared by varying the G:N ratio from 0.2 to 1.5. Figure 1 shows the X-ray diffractograms obtained on different  $\text{Li}(\text{Ni}_{1/3}\text{Co}_{1/3}\text{Mn}_{1/3})\text{O}_2$  powder samples prepared with different G:N ratios. In this figure, the corresponding standard diffraction pattern of the  $\text{Li}(\text{Ni}_{1/3}\text{Co}_{1/3}\text{Mn}_{1/3})\text{O}_2$  phase is labeled as 333 (Samarasingha *et al.*, 2008). Accordingly, the existence of only the appropriate R-3m phase of  $\alpha$ - $\text{NaFeO}_2$  layered structure of  $\text{Li}(\text{Ni}_{1/3}\text{Co}_{1/3}\text{Mn}_{1/3})\text{O}_2$  is seen in all these powder samples prepared in this study with different G: N ratios.

Furthermore, as seen in Figure 1, this study reveals the possibility of obtaining the appropriate  $\text{Li}(\text{Ni}_{1/3}\text{Co}_{1/3}\text{Mn}_{1/3})\text{O}_2$  phase even at a very low G:N ratio such as 0.2. However, increase of the G:N ratio up to 0.8 has clearly improved the crystal structure of the material evidenced by the well defined sharper and narrower peaks seen in the diffractograms. However, further increase of G:N ratio caused a slight degradation of the  $\text{Li}(\text{Ni}_{1/3}\text{Co}_{1/3}\text{Mn}_{1/3})\text{O}_2$  structure with the visible gradual reduction of splitting of (006)/(102) and (108)/(110)

diffraction peaks. It also created a slightly broader and less defined peaks at these high G:N ratios. By considering these factors, the G:N ratio of 0.6 seems to result in the optimum crystal structure of  $\text{Li}(\text{Ni}_{1/3}\text{Co}_{1/3}\text{Mn}_{1/3})\text{O}_2$  with highly defined narrow peaks and appropriate peak splitting.

### Particle properties

The Scanning Electron Microscopic (SEM) study performed on the prepared  $\text{Li}(\text{Ni}_{1/3}\text{Mn}_{1/3}\text{Co}_{1/3})\text{O}_2$  samples shows the existing of quasi-spherical, sub-micron level soft agglomerates in the size range between 10 and 75  $\mu\text{m}$ . These agglomerates seems to be formed by the softly aggregating nanoscale primary particles. These primary particles are rather spherical in shape, with 50 to 200 nm diameter in size. A direct evidence for this is given in the SEM image (Figure 2) obtained on  $\text{Li}(\text{Ni}_{1/3}\text{Mn}_{1/3}\text{Co}_{1/3})\text{O}_2$  sample prepared with G:N = 0.6. It was also observed that the spherical shaped secondary particles composed of primary particles of around 200 nm, that can be an ideal particle morphology for a greater integrated electrochemical performance (Liu *et al.*, 2014; Ren, 2009). Therefore, a favorable electrochemical performance in the Li-ion cells can be expected with  $\text{Li}(\text{Ni}_{1/3}\text{Mn}_{1/3}\text{Co}_{1/3})\text{O}_2$  material prepared in this study by GNC process. Furthermore, as seen in Figure 3, the Energy Dispersive Spectra (EDS) analysis performed on this synthesized  $\text{Li}(\text{Ni}_{1/3}\text{Mn}_{1/3}\text{Co}_{1/3})\text{O}_2$  shows the presence of only the Ni, Co, Mn and O (Li could

not be detected by EDS). The Ni:Co:Mn atomic ratio calculated based on this EDS result is approximately equal to 1:1:1.

Figure 4 shows the thermogravimetric and differential thermogravimetric (dW/dT) plots obtained for  $\text{Li}(\text{Ni}_{1/3}\text{Co}_{1/3}\text{Mn}_{1/3})\text{O}_2$  samples prepared with different G: N ratios of 0.2, 0.4, 0.6, and 1.0. It can be seen that in the Thermogravimetric Analysis (TGA), the weight loss takes place in three steps and they are comparable with those found in literature (Kabi and Ghosh, 2013). The first plateau of weight loss seen in between 100 °C and 200 °C is very likely due to the loss of water molecules (Kabi and Ghosh, 2013). The  $\text{Li}(\text{Ni}_{1/3}\text{Co}_{1/3}\text{Mn}_{1/3})\text{O}_2$  samples prepared with different G:N ratios at 0.2 and 1.0 show the exothermic peaks at 206 °C and 244 °C, corresponding to the weight losses of 0.5 wt% and 0.2 wt%, respectively. There was no significant exothermic peak to be seen within this region for the remaining  $\text{Li}(\text{Ni}_{1/3}\text{Mn}_{1/3}\text{Co}_{1/3})\text{O}_2$  samples, presumably due to their better thermal stability. From the XRD analysis conducted on  $\text{Li}(\text{Ni}_{1/3}\text{Mn}_{1/3}\text{Co}_{1/3})\text{O}_2$  at high temperature, Nam *et al* has reported that the structural changes of this material starts around 170 °C and the phase transition takes place gradually up to 600 °C (Nam, *et al.*, 2009). Therefore, the weight losses corresponding to exothermic peaks at temperatures from 100 °C to 550 °C seen in this study, may be due to the combined effect of loss of absorbed water molecules and structural phase transition.

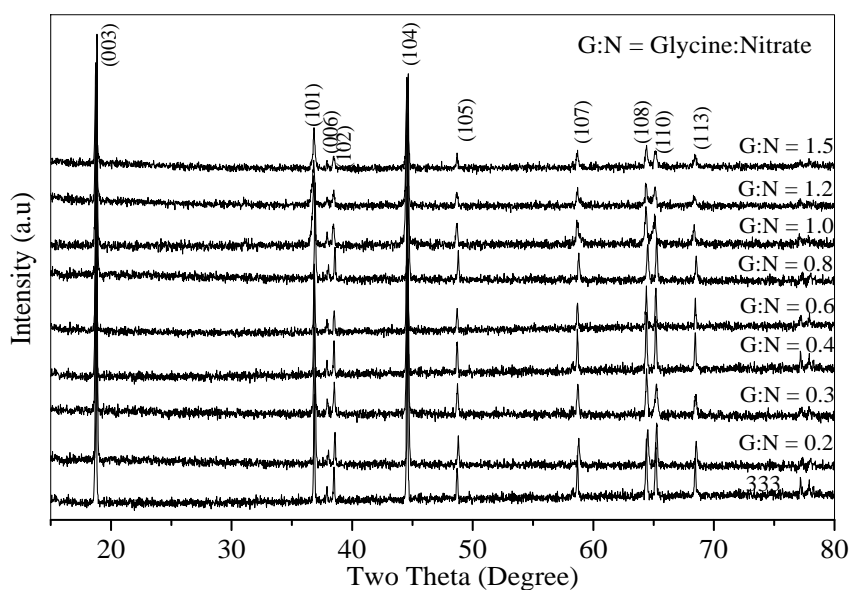


**Figure 1:** X-ray diffractograms obtained on different  $\text{Li}(\text{Ni}_{1/3}\text{Co}_{1/3}\text{Mn}_{1/3})\text{O}_2$  samples prepared with different G:N ratios from 0.2 to 1.5. The standard diffraction pattern of  $\text{Li}(\text{Ni}_{1/3}\text{Co}_{1/3}\text{Mn}_{1/3})\text{O}_2$  phase is labeled as 333 (Samarasingha *et al.*, 2008).

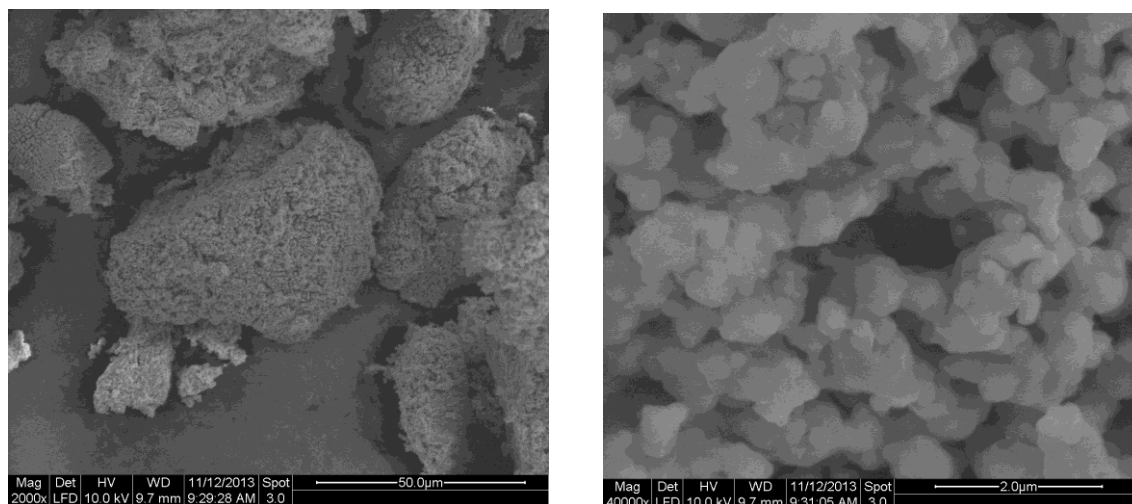


**Figure 2:** SEM images of  $\text{Li}(\text{Ni}_{1/3}\text{Co}_{1/3}\text{Mn}_{1/3})\text{O}_2$  prepared with G:N = 0.6, at different magnifications.

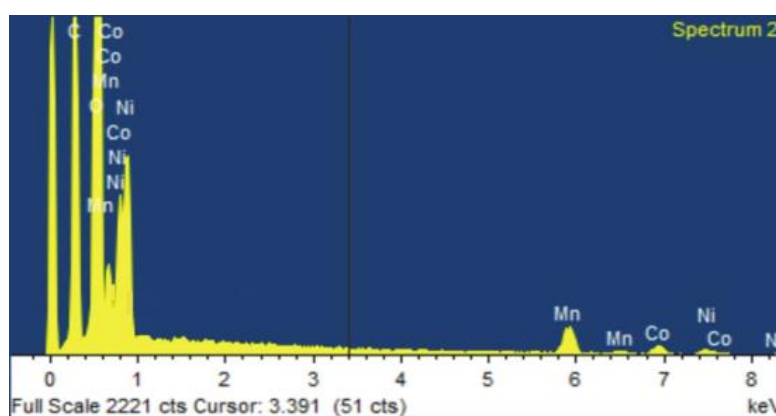


**Figure 3:** EDS spectra of  $\text{Li}(\text{Ni}_{1/3}\text{Co}_{1/3}\text{Mn}_{1/3})\text{O}_2$  prepared with G:N = 0.6

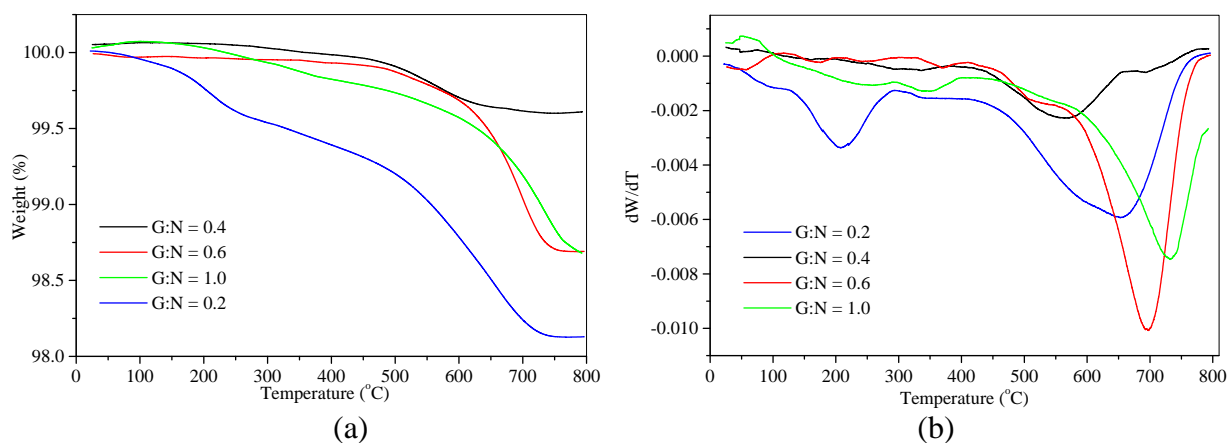


**Figure 4:** (a) Thermogravimetric and (b) Differential thermogravimetry (dW/dT) plots obtained on the  $\text{Li}(\text{Ni}_{1/3}\text{Co}_{1/3}\text{Mn}_{1/3})\text{O}_2$  samples prepared with different G:N ratios.

The third step of the weight loss occurs between 550 °C and 760 °C resulting prominent exothermic peak in dW/dT plots due to the release of oxygen depending on its structural stability (Kabi and Ghosh, 2013). It can be clearly seen in the Figure 4 (b) that the exothermic peak had shifted to low temperatures for  $\text{Li}(\text{Ni}_{1/3}\text{Mn}_{1/3}\text{Co}_{1/3})\text{O}_2$  synthesized with low

G:N ratios, indicating their lesser structural stability compared to those prepared with high G:N ratios. The material prepared with G:N = 0.2 shows existence of the exothermic peak at 650 °C, corresponding to weight losses of 1.5 wt%. Even though the  $\text{Li}(\text{Ni}_{1/3}\text{Co}_{1/3}\text{Mn}_{1/3})\text{O}_2$  prepared with the G:N = 0.4 reported the lowest weight loss, it is more thermally unstable since it has

liberated oxygen at lower temperature. Moreover,  $\text{Li}(\text{Ni}_{1/3}\text{Co}_{1/3}\text{Mn}_{1/3})\text{O}_2$  prepared with higher G:N ratios of 0.6 and 1.0 show existence of the exothermic peaks at 700 °C and 733 °C, corresponding to weight losses of 1.2 wt% and 1.3 wt%,. Accordingly,  $\text{Li}(\text{Ni}_{1/3}\text{Co}_{1/3}\text{Mn}_{1/3})\text{O}_2$  synthesized at the G:N ratio of 0.6 can be regarded as most thermally stable sample in this study.

Altogether, the crystal structure as evidenced by XRD analysis, and particle size and morphology evidenced by SEM, clearly indicate that G:N ratio of 0.6 resulted the  $\text{Li}(\text{Ni}_{1/3}\text{Co}_{1/3}\text{Mn}_{1/3})\text{O}_2$  with optimum powder morphology and appropriate crystal structure by the GNC process. Thermal characterization also reveals that the  $\text{Li}(\text{Ni}_{1/3}\text{Co}_{1/3}\text{Mn}_{1/3})\text{O}_2$  synthesized with G:N ratio of 0.6 is thermally more stable. Therefore, G:N ratio of 0.6 was selected as the optimum G:N ratio for the synthesis of the  $\text{Li}(\text{Ni}_{1/3}\text{Co}_{1/3}\text{Mn}_{1/3})\text{O}_2$  and its derivatives by the GNC process.

#### Powder densification and electrical characterization

Figure 5 shows the variation of both the green density (density before sintering) and the sintered density (density after heat treating) of the pellets pressed at different pressures by the cold uni-axial pressing technique. As seen in the figure, the green density is continuously increasing with the pressing pressure, due to better packing of powder particles in the green body under the higher pressures. However, the behavior of the sintered density with pressing pressure is considerably different. With the increase of the pressing pressure, the sintered pellet density has increased to a maximum at around 250 MPa of

applied pressure. Then sintered density started to decrease with increase of pressure. This could be due to the formation of internal cracking in the green body under extremely higher pressures applied on it, resulting a weaker packing. The formed internal cracks extend during the following heating and cooling process, and create higher internal porosity, that lowers the strength of the final sintered body. This higher internal porosity together with the internally fractured structure had already made the pellet inferior to be used for any meaningful characterization or application. Hence, applied pressure of 250 MPa, which resulted a well sintered solid body with the highest sintered density, was selected as the optimum pressing pressure for this material.

The electrical conductivity of the prepared dense sintered pellets of  $\text{Li}(\text{Ni}_{1/3}\text{Mn}_{1/3}\text{Co}_{1/3})\text{O}_2$  samples was measured by the d.c. four probe technique. Figure 6 shows the d.c. electrical conductivity behaviour of these  $\text{Li}(\text{Ni}_{1/3}\text{Mn}_{1/3}\text{Co}_{1/3})\text{O}_2$  samples prepared with different G:N ratio. The electrical conductivity increases exponentially with the increasing temperature indicating the semiconducting nature of the material (Wijayasinghe, 2006). The room temperature d.c. conductivity of these all synthesized samples are in the order of  $10^{-7} \text{ S cm}^{-1}$  (see Table 1). The d.c. conductivity of the  $\text{Li}(\text{Ni}_{1/3}\text{Mn}_{1/3}\text{Co}_{1/3})\text{O}_2$  synthesized by the GNC process in this study is lower by two orders of magnitude to that reported for the same material synthesized by the Pechini method (Samarasingha et al., 2008; Samarasingha et al., 2014). This decrease in electrical conductivity may be related to the morphological difference of the  $\text{Li}(\text{Ni}_{1/3}\text{Mn}_{1/3}\text{Co}_{1/3})\text{O}_2$  materials prepared by the two different synthesis methods.

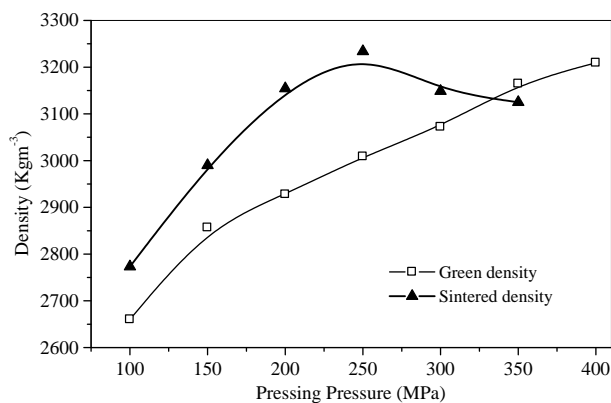


**Figure 5:** Variation of green density and sintered density of  $\text{Li}(\text{Ni}_{1/3}\text{Co}_{1/3}\text{Mn}_{1/3})\text{O}_2$  pellets pressed at different pressing pressures, under cold uni-axial pressing.

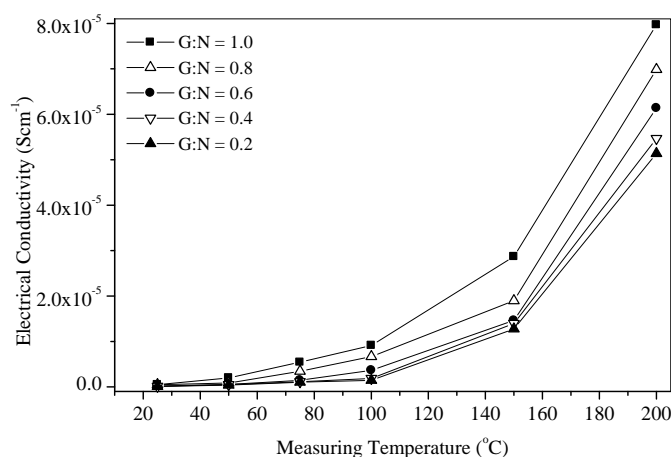


**Figure 6:** The temperature dependence of d.c. electrical conductivity of  $\text{Li}(\text{Ni}_{1/3}\text{Mn}_{1/3}\text{Co}_{1/3})\text{O}_2$  prepared with different G:N ratios.

**Table 1:** Electrical conductivity of  $\text{Li}(\text{Ni}_{1/3}\text{Co}_{1/3}\text{Mn}_{1/3})\text{O}_2$  materials synthesized with different G: N ratios.

Glycine: Nitrate ratio (G:N)	0.2	0.4	0.6	0.8	1.0
Electrical conductivity at 25 °C ( $\text{S cm}^{-1}$ )	$1.0 \times 10^{-7}$	$1.2 \times 10^{-7}$	$2.1 \times 10^{-7}$	$4.9 \times 10^{-7}$	$5.0 \times 10^{-7}$

So far, this study revealed that the GNC process is a promising method to synthesize phase pure  $\text{Li}(\text{Ni}_{1/3}\text{Mn}_{1/3}\text{Co}_{1/3})\text{O}_2$ . The main advantage of this method is the possibility of synthesizing the desired highly crystalline material within a short calcination period. Furthermore, the resulting particle morphology consists of nanoscale primary particles with high surface area, aggregated to form micron size secondary particles. This is expected to be much more favorable for improving the electrochemical performance of the  $\text{Li}(\text{Ni}_{1/3}\text{Mn}_{1/3}\text{Co}_{1/3})\text{O}_2$  as a cathode material in LIB.

Under a further study, galvanostatic cycling of a coin cell assembled with this fabricated  $\text{Li}(\text{Ni}_{1/3}\text{Mn}_{1/3}\text{Co}_{1/3})\text{O}_2$  cathode as the working electrode and Li foil as counter and reference electrodes, were carried out between 2.5 - 4.6 V, at a current density of 0.2 C (1 C =  $140 \text{ mA g}^{-1}$ ). In a previous study, phase pure  $\text{Li}(\text{Ni}_{1/3}\text{Co}_{1/3}\text{Mn}_{1/3})\text{O}_2$  was reported to be synthesized by the Pechini method followed by calcination at 900 °C for four hours (Samarasingha *et al.*, 2008). The microstructure of that material was a sponge like agglomerate composed of large primary particles in the range 0.8 - 1.0  $\mu\text{m}$ . That material reported an initial discharge capacity of 160  $\text{mAh g}^{-1}$  at C/5 rate between 3.0 - 4.5 V (Samarasingha *et al.*, 2008).

More interestingly, our  $\text{Li}(\text{Ni}_{1/3}\text{Co}_{1/3}\text{Mn}_{1/3})\text{O}_2$  material synthesized in this study by GNC method, showed a significantly higher initial discharge capacity of 187  $\text{mAh g}^{-1}$  at C/5 rate between 2.5 V and 4.6 V. After the tenth cycle, the irreversible capacity decreased to 3.2  $\text{mAh g}^{-1}$  with coulombic efficiency of 97.9%. This significantly better performance, resulted in the present study, can be attributed to success of obtaining appropriate powder particle morphology. Therefore, this study reveals the successful optimization of the GNC process to synthesize  $\text{Li}(\text{Ni}_{1/3}\text{Co}_{1/3}\text{Mn}_{1/3})\text{O}_2$  with appropriate microstructure for improved cathode performance in LIB.

## CONCLUSIONS

Phase-pure  $\text{Li}(\text{Ni}_{1/3}\text{Co}_{1/3}\text{Mn}_{1/3})\text{O}_2$  was successfully synthesized by the Glycine-Nitrate Combustion (GNC) process with different Glycine to Nitrate ratios (G:N) in the range 0.2 - 1.5, with a shorter calcination time of two hours. The increase of the G:N ratio decreased the size of the resultant powder particles to nano-scale. Further, the thermogravimetric study revealed that  $\text{Li}(\text{Ni}_{1/3}\text{Mn}_{1/3}\text{Co}_{1/3})\text{O}_2$  prepared with G:N = 0.6 as the most thermally stable material. Therefore, this study suggests the optimum value of 0.6 for the G:N ratio to obtain phase pure, well crystalline  $\text{Li}(\text{Ni}_{1/3}\text{Mn}_{1/3}\text{Co}_{1/3})\text{O}_2$  with rather spherical shaped micron size secondary particles

formed by the softly agglomerated primary particles of 200 - 300 nm. The electrical conductivity measured on the dense sintered  $\text{Li}(\text{Ni}_{1/3}\text{Mn}_{1/3}\text{Co}_{1/3})\text{O}_2$  materials by the dc four-probe technique showed the semiconducting nature with dc conductivity in the order of  $10^{-7}$  S  $\text{cm}^{-1}$  at 25 °C. The lithium ion half cell prepared with this cathode material showed initial discharge capacity of 187  $\text{mAhg}^{-1}$  with 25  $\text{mAh g}^{-1}$  irreversible capacity at cut-off voltage of 2.5 - 4.6 V at 25 °C. After the tenth cycle, the irreversible capacity decreased to 3.2  $\text{mAhg}^{-1}$  with coulombic efficiency was maintained at 97.9%. Altogether, this study reveals successful use of GNC process to prepare  $\text{Li}(\text{Ni}_{1/3}\text{Co}_{1/3}\text{Mn}_{1/3})\text{O}_2$  with highly favorable powder morphology for the LIB cathode application.

---

#### ACKNOWLEDGEMENT

Mr. W. G. Jayasekara of the National Institute of Fundamental Studies, Kandy, Sri Lanka is gratefully acknowledged for the support given throughout this study.

---

#### REFERENCES

- Chick, L.A., Pederson, L.R., Maupin, G.D., Bates, J.L., Thomas, L.E. and Exarhos, G.J. (1990). Glycine-nitrate combustion synthesis of oxide ceramic powders. *Materials Letters*. **10(1, 2)**:6-12.
- Kabi, S. and Ghosh, A. (2013). Microstructure of  $\text{Li}(\text{Mn}_{1/3}\text{Ni}_{1/3}\text{Co}_{1/3})\text{O}_2$  cathode material for lithium ion battery: Dependence of crystal structure on calcination and heat-treatment temperature. *Materials Research Bulletin*. **48**:3405-3410.
- Liu, J., Chen, H., Xie, J., Sun, Z., Wu, N. and Wu, B. (2014). Electrochemical performance studies of Li-rich cathode materials with different primary particle sizes. *Journal of Power Sources*. **251**: 208-214.
- Nam, K.-W., Yoon, W.-S. and Yang, X.-Q. (2009). Structural changes and thermal stability of charged  $\text{LiNi}_{1/3}\text{Co}_{1/3}\text{Mn}_{1/3}\text{O}_2$  cathode material for Li-ion batteries studied by time-resolved XRD. *Journal of Power Sources*. **189(1)**:515-518.
- Oljaca, M., Blizanac, B.A., Pasquier, D., Sun, Y., Bontchev, R., Suszko, A., Wall, R. and Koehlert, K. (2014). Novel  $\text{Li}[\text{Ni}_{1/3}\text{Co}_{1/3}\text{Mn}_{1/3}]\text{O}_2$  cathode morphologies for high power Li-ion batteries. *Journal of Power Sources*. **248**: 729-738.
- Patoux, S. and Doeff, M.M. (2004). Direct synthesis of  $\text{Li}(\text{Ni}_{1/3}\text{Co}_{1/3}\text{Mn}_{1/3})\text{O}_2$  from nitrate precursors. *Electrochemistry Communications*. **6**:767-772.
- Ren, H., Huang, Y., Wang, Y., Li, Z., Cai, P., Peng, Z. and Zhou, Y. (2009). Effects of different carbonate precipitators on  $\text{Li}(\text{Ni}_{1/3}\text{Co}_{1/3}\text{Mn}_{1/3})\text{O}_2$  morphology and electrochemical performance. *Materials Chemistry and Physics*. **117**:41-45.
- Samarasingha, P.B., Wijayasinghe, A., Behm, M., Dissanayake, L. and Lindbergh, G. (2014). Development of cathode materials for lithium ion rechargeable batteries based on the system  $\text{Li}(\text{Ni}_{1/3}\text{Mn}_{1/3}\text{Co}_{(1/3-x)}\text{M}_x)\text{O}_2$ , (M = Mg, Fe, Al and  $x = 0.00$  to 0.33). *Solid State Ionics*. **268(B)**:226-230.
- Samarasingha, P., Tran-Nguyena, D.-H., Behma, M. and Wijayasinghe, A. (2008).  $\text{Li}(\text{Mn}_{1/3}\text{Ni}_{1/3}\text{Co}_{1/3})\text{O}_2$  synthesized by the Pechini method for the positive electrode in Li-ion batteries: Material characteristics and electrochemical behavior. *Electrochimica Acta*. **53**:7995-8000.
- Shi, S.J., Tu, J.P., Tang, Y.Y., Yu, Y.X., Zhang, Y.Q., Wang, X.L. and Gu, C.D., (2013). Combustion synthesis and electrochemical performance of  $\text{Li}[\text{Li}_{0.2}\text{Mn}_{0.54}\text{Ni}_{0.13}\text{Co}_{0.13}]\text{O}_2$  with improved rate capability. *Journal of Power Sources*. **228**:14-23.
- Wijayasinghe, A., Bergman, B. and Lagergren, C. (2006).  $\text{LiFeO}_2$ - $\text{LiCoO}_2$ - $\text{NiO}$  materials for Molten Carbonate Fuel Cell cathodes. Part I: Powder synthesis and material characterization. *Solid State Ionics*. **177**:165-173.
- Wilcox, J., Patoux, S. and Doeff, M. (2009). Structure and Electrochemistry of  $\text{Li}(\text{Ni}_{1/3}\text{Co}_{1/3-y}\text{M}_y\text{Mn}_{1/3})\text{O}_2$  (M = Ti, Al, Fe) Positive Electrode Materials. *Journal of The Electrochemical Society*. **156(3)**: A192-A198.
- Zhang, S. (2007). Characterization of high tap density  $\text{Li}[\text{Ni}_{1/3}\text{Co}_{1/3}\text{Mn}_{1/3}]\text{O}_2$  cathode material synthesized via hydroxide co-precipitation. *Electrochimica Acta*. **52(25)**: 7337-7342.
-

